Naunyn-Schmiedeberg's Arch Pharmacol
DOI 10.1007/s00210-017-1421-0

ORIGINAL ARTICLE

Cativic acid-caffeic acid hybrid exerts cytotoxic effects and induces apoptotic death in human neuroblastoma cells

Natalia P. Alza[1,2] · **Ana P. Murray**[2] · **Gabriela A. Salvador**[1]

Received: 19 April 2017 / Accepted: 23 August 2017

Abstract The development of hybrids from natural products is a promising strategy for drug discovery. In cancer therapy, there is a need to discover novel agents that can induce apoptosis in cancer cells. To contribute to this field of interest, we investigated the effect of a synthetic hybrid from cativic acid and caffeic acid (**5**) on viability, proliferation, and apoptosis in human neuroblastoma cells (IMR-32). Three hybrids were prepared via Mitsunobu esterification from 17-hydroxycativic acid (**1**) and natural phenols. Cell viability was analyzed by MTT assay. SYTOX green and LDH leakage were used to determine the cytotoxic effect. Caspase-3 activity, cell cycle phases, and proliferation were analyzed in order to characterize the biological effects of hybrid **5**. The mitogen-activated protein kinase (MAPK) status was evaluated for elucidating the potential mechanisms involved in hybrid **5** effect. Hybrid **5** reduced the viability of IMR-32 cells in a time- and concentration-dependent manner (IC_{50} = 18.0 ± 1.3 μM) as a result of its antiproliferative effect through changes in the cell cycle distribution and induction of apoptosis associated with activation of caspase-3. Exposure to **5** triggered ERK1/2 activation and nuclear translocation. Hybrid **5** also promoted an increase in nuclear localization of the transcription factor c-Jun. Inhibition of ERK1/2 and JNK potentiated **5**-induced inhibition of IMR-32 viability. Hybrid **5** displays cell growth inhibition by promoting cell cycle arrest and apoptosis, through ERK1/2 and JNK participation.

Keywords Hybrids · Cativic acid · Human neuroblastoma · Apoptosis · MAPK

Introduction

Natural products (NP) play a leading role in drug discovery and development as the source of therapeutic products, especially as anticancer and anti-infective agents (Newman and Cragg 2016). A range of hybrids is possible to develop from a limited number of NP, which could be in the millions, each hybrid exhibiting inherent biological activities that may be different from the original monomers (Berube 2016; Tietze et al. 2003). The development of artificial hybrids from NP has therefore emerged as a novel approach in the field of drug discovery (Tietze et al. 2003).

Labdanes are characteristic constituents of *Grindelia* (Asteraceae) (Mahmoud et al. 2000; Hoffmann et al. 1988; Ahmed et al. 2001), a genus represented in South America by 26 species (Zuloaga et al. 2008). In a previous study, we isolated 17-hydroxycativic acid (**1**) using a bioassay-guided fractionation of the ethanolic extract of *Grindelia ventanensis* which showed in vitro acetylcholinesterase inhibitory activity (Alza et al. 2014). To enhance this activity, a series of derivatives of **1** were prepared by simple transformations in the carboxylic group, introducing a C2-C6 linker and a tertiary amine group.

Electronic supplementary material The online version of this article (https://doi.org/10.1007/s00210-017-1421-0) contains supplementary material, which is available to authorized users.

✉ Gabriela A. Salvador
salvador@criba.edu.ar

[1] Instituto de Investigaciones Bioquímicas de Bahía Blanca, Departamento de Biología, Bioquímica y Farmacia, Universidad Nacional del Sur y Consejo Nacional de Investigaciones Científicas y Técnicas, Camino La Carrindanga km 7, 8000 Bahía Blanca, Argentina

[2] Instituto de Química del Sur, Departamento de Química, Universidad Nacional del Sur y Consejo Nacional de Investigaciones Científicas y Técnicas, Av. Alem 1253, 8000 Bahía Blanca, Argentina

Published online: 05 September 2017

In the present study, we analyzed the effect of labdane **1** and three semisynthetic hybrids (**3**–**5**) with the natural phenols coniferyl alcohol, ferulic acid, and caffeic acid, respectively, on a cell line derived from human neuroblastoma (IMR-32). Cytotoxicity, antiproliferative effect, and apoptosis induction of hybrid **5** were also investigated along with the regulation of MAPK signaling pathways.

Materials and methods

Chemistry

General procedures and materials

NMR spectra were recorded with a Bruker ARX300 spectrometer operated at 300 and 75 MHz for ^{1}H and ^{13}C, respectively, in $CDCl_3$. High-resolution mass spectra (HRMS) were obtained on a QTOF mass spectrometer (micrOTOF-QII Series, Bruker). UV spectra were recorded on a JASCO-V630BIO spectrophotometer. All derivatives were rigorously characterized by NMR spectroscopy and mass spectrometry. Compounds **2**–**5** are described here for the first time and 2D NMR spectra were used for the unequivocal assignments (Table 1 and Supplementary material). Log *P* values were estimated using ChemDraw Ultra 11.

Plant material

Aerial parts of *G. ventanensis* were collected from Sierra de la Ventana, Province of Buenos Aires, Argentina (November 2014). A voucher specimen was identified by Dr. María Gabriela Murray and deposited under the label Murray, M.G. 546, in Herbarium BBB of the Universidad Nacional del Sur, Bahía Blanca, Argentina.

*Extraction and isolation of 17-hydroxycativic acid (**1**)*

Compound **1** was isolated and identified by ^{1}H and ^{13}C NMR as previously described, with slight modifications (Alza et al. 2014). Briefly, dry ethanolic extract (90.0 g) of aerial parts of *G. ventanensis* (980.0 g) was subjected to column chromatography (CC) on Silica gel 60 (70–230 mesh, 800.0 g) eluting with mixtures of hexane/EtOAc. From the fractions eluted with hexane/EtOAc 50:50 (vol/vol) and hexane/EtOAc 40:60 (vol/vol), **1** crystallized spontaneously (1.7 g of **1**, 0.17% w/w of plant material).

*Preparation of compound **2***

Compound **1** (2.0 mmol) and K_2CO_3 (4.0 mmol) were added to DMF (23.5 ml) and stirred at RT for 10 min, after which ICH_3 (8.0 mmol) was added. The reaction mixture was stirred for another 24 h and subsequently evaporated to dryness. The residue was subjected to CC on silica gel with hexane/EtOAc. Fractions eluted with hexane/EtOAc 80:20 (vol/vol) afforded methyl ester **2** (591.4 mg, 1.8 mmol, yield 86.0%).

Table 1 ^{1}H and ^{13}C NMR spectroscopic data for hybrids **3**–**5** in $CDCl_3$, δ in parts per million

	3		**4**		**5**	
	δ(C)	δ(H)	δ(C)	δ(H)	δ(C)	δ(H)
1	39.2	1.85 os 0.97 os	39.2	1.87 os 1.00 os	39.2	1.85 os 0.98 os
2	18.9	1.47 os	18.9	1.48 os	18.9	1.47 os
3	42.4	1.41 os 1.15 os	42.4	1.43 *m* 1.17 os	42.4	1.41 *m* 1.18 os
4	33.2		33.1		33.1	
5	50.1	1.21 os	49.9	1.26 os	49.9	1.24 os
6	23.8	2.05 os 1.96 os	24.0	2.10 os 1.93 os	24.0	2.09 os 1.94 os
7	125.7	5.74 *m*	129.0	5.85 *m*	129.2	5.85 *m*
8	139.4		134.4		134.3	
9	52.6	1.77 os	52.8	1.81 os	52.8	1.79 os
10	37.0		37.0		37.1	
11	24.4	1.50 os 1.20 os	24.0	1.52 os 1.21 os	24.1	1.51 os 1.20 os
12	38.7	1.50 os 1.19 os	38.7	1.52 os 1.21 os	38.8	1.53 os 1.19 os
13	31.5	1.96 os	31.2	1.94 os	31.3	1.93 os
14	41.6	2.36 *dd* 2.20 *dd*	41.4	2.32 *dd* 2.09 os	41.6	2.33 *dd* 2.10 os
15	173.4		173.8		174.2	
16	20.1	0.98 *d*	20.1	0.94 *d*	20.0	0.94 *d*
17	66.0	4.12 *d* 3.95 *d*	67.7	4.68 *d* 4.55 *d*	68.0	4.68 *d* 4.56 *d*
18	33.2	0.85 *s*	33.2	0.86 *s*	33.2	0.86 *s*
19	22.1	0.88 *s*	21.9	0.89 *s*	22.0	0.89 *s*
20	13.8	0.74 *s*	13.8	0.78 *s*	13.8	0.77 *s*
21			51.5	3.62 *s*	51.7	3.63 *s*
1′	65.3	4.71 *dd*	167.1		167.4	
2′	121.1	6.14 *dt*	115.8	6.30 *d*	116.0	6.27 *d*
3′	134.6	6.58 *d*	145.0	7.61 *d*	144.9	7.57 *d*
4′	129.0		127.2		127.8	
5′	108.6	6.93 os	109.5	7.06 os	114.5	7.12 br *s*
6′	146.8[a]		148.1[a]		146.4[a]	
7′	146.1[a]		146.9[a]		143.9[a]	
8′	114.6	6.87 os	114.8	6.91 *d*	115.6	6.87 *d*
9′	120.8	6.91 os	123.2	7.08 os	122.6	7.00 *d*
10′	56.1	3.91 *s*	56.1	3.93 *s*		

os: overlapped signal; *s*: singlet; *br s*: broad singlet; *d*: doublet; *dd*: doublet of doublets; *dt*: doublet of triplets; *m*: multiplet

[a] Interchangeable signals

General preparation of hybrids **3**–**5**

Compounds **3**–**5** were prepared by the Mitsunobu protocol (Appendino et al. 2002). Triphenylphosphine 0.15–0.2 mmol) and diisopropyl azodicarboxylate (0.15–0.2 mmol) were added to a cooled (0 °C) solution of alcohol (0.1–0.2 mmol) and the corresponding acid (0.15–0.3 mmol) in dry THF (2 ml). For preparation of hybrid **3**, 29.4 mg of coniferyl alcohol and 102.7 mg of **1** were used. Hybrids **4** and **5** were obtained from **2** (34.0 and 62.2 mg, respectively) and ferulic and caffeic acid (29.3 and 54.2 mg, respectively). The reaction mixture was stirred at RT for 48 h, worked up by removal of THF, dissolved on EtOAc, and extracted with saturated $NaHCO_3$. The organic phase was washed with brine, dried ($MgSO_4$), and evaporated. The crude reaction was subjected to CC on Silica gel 60 (200–425 mesh) with DCM/MeOH 99:1 (vol/vol) as eluent to obtain hybrids **3** (5.7 mg) and **5** (12.6 mg) or with DCM to obtain hybrid **4** (25.2 mg). The purity of compounds **3**–**5** was determined by HPLC (95.1, 97.5, and 98.0%, respectively).

Biological assays

Cell culture

IMR-32 was obtained from ATCC. HCT-116 and MDA-MB 231 were kindly provided by Dr. Maria Marta Facchinetti and Dr. Alejandro Curino (INIBIB-CONICET). Cells were cultured in Dulbecco's high-glucose modified Eagle's medium (DMEM, Gibco, Thermo Fisher Scientific, Argentina) supplemented with 10% fetal bovine serum (FBS, Natocor, Argentina), 100 U/ml penicillin, 100 μg/ml streptomycin, and 0.25 μg/ml amphotericin B (Gibco, Thermo Fisher Scientific, Argentina) at 37 °C in humidified atmosphere containing 5% CO_2. Prior to treatments, the medium was replaced by serum-free medium.

Cell viability assay

The MTT reduction assay was used to assess cell viability. Metabolically, viable cells reduce water-soluble tetrazolium salt, MTT, to a colored, water-insoluble formazan salt. Cells were seeded in 96-well plates at a density of 5000 cells/well and, 24 h later, were treated with different concentrations ranging from 0.5 to 50 μM of the tested compounds. After 24, 48, or 72 h of incubation, MTT (5 mg/ml in PBS) was added to the medium (final concentration 0.5 mg/ml). The assay was stopped after incubation for 2 h at 37 °C in a 5% CO_2 atmosphere. The viable cell number was correlated with formazan production, which was dissolved with 20% SDS (pH 4.7) and measured spectrophotometrically at 570 and 650 nm in the microplate spectrophotometer (Multiskan GO, Thermo Scientific). IC_{50} values were calculated by nonlinear regression analysis using GraphPad Prism 5.

SYTOX green nucleic acid stain

SYTOX green, a DNA-binding dye, is a useful indicator of dead cells within a population because it only enters cells with a compromised plasma membrane and becomes fluorescent when bound to nucleic acid. Cells were grown onto glass coverslips and incubated with 10–25 μM **5** overnight. They were subsequently treated with SYTOX green dye for 15 min at RT (final concentration 1 μM), rinsed 3 times in PBS, and fixed with 4% paraformaldehyde. Nuclei were counterstained with Hoechst. Coverslips were mounted and slides were observed in the fluorescence microscope.

Measurement of LDH release

LDH leakage was determined as previously described (Uranga et al. 2009), with slight modifications. IMR-32 cells were treated with 10–25 μM **5**, and after 24 h, the incubation medium was collected and centrifuged (1000×*g* for 10 min at 4 °C). The resulting supernatant was used to determine LDH activity, which was measured spectrophotometrically using an LDH-P UV AA kit. Briefly, the conversion rate of reduced nicotinamide adenine dinucleotide to oxidized nicotinamide adenine dinucleotide was followed at 340 nm.

BrdU immunofluorescence assay

IMR-32 cells were seeded on glass coverslips. After treatment with 10, 15, and 20 μM **5** for 12 and 24 h, 5-bromo-2-deoxyuridine (BrdU; Sigma) was added (final concentration 1 μM) and the cells were incubated for 150 min. They were then washed with DMEM, fixed for 30 min in cold 70% ethanol (−20 °C), incubated with 2 N HCl for 10 min at RT, and finally washed with PBS followed by incubation with a borate solution (1:1 ratio of A:B; A: 1.9 g/100 ml borax; B: 1.3 g/100 ml boric acid) for 10 min at RT. Cells were further incubated with a primary sheep antibody against BrdU (1:200, Biodesign International) overnight at 4 °C and subsequently incubated with anti-sheep-Alexa 594 (1:300, Molecular Probes) for 1 h at RT. After DAPI staining, coverslips were mounted and slides were observed in the fluorescence microscope. The percentage of BrdU-positive cells was calculated in 10 microscopic fields of three different experiments.

Cell cycle analysis by flow cytometry

Approximately 1.2×10^6 IMR-32 cells were incubated with or without 10–20 μM **5** for 24 and 72 h. Cells were removed with PBS/EDTA followed by centrifugation (800×*g* at 4 °C for 5 min). After being washed once with PBS, cells were

resuspended in 300 μl of PBS, fixed with 700 μl of cold ethanol (70%) for 1 h, rewashed with PBS, and centrifuged as above. After suspending the cell pellet in 500 μl of PBS, 5 μl of 10 mg/ml RNase A was added and the pellet was incubated at 37 °C for 30 min. Finally, 10 μl of 1 mg/ml of propidium iodide (PI) was subsequently added (final concentration 10 μg/ml). DNA content of cells was analyzed using a flow cytometer (FACSCalibur, Becton Dickinson, CA, USA).

Caspase-3 activity

Caspase-3 activity was assessed following Hanzel and Verstraeten (Hanzel and Verstraeten 2009) with minor modifications. Briefly, IMR-32 cells were grown on 35-mm diameter cell culture dishes and incubated at 37 °C for 8 h with or without the addition of 10–25 μM **5**. Cells from two dishes were scraped into PBS and centrifuged (10 min at 1000×*g* at 4 °C). Pellets were suspended in a 50 mM HEPES buffer (pH 7.4) containing 0.1% NP-40, 1 mM dithiothreitol (DTT), 0.1 mM EDTA, and 150 mM NaCl and incubated on ice for 5 min. Samples were centrifuged (12,000×*g* for 10 min at 4 °C). Protein content was measured in supernatants (Bradford 1976). Supernatants containing 150–200 μg protein were incubated in the presence of 10% (*v*/*v*) glycerol and 0.2 mM of caspase-3 chromogenic substrate (Ac-DEVD-pNA) overnight at 37 °C. The formation of *p*-nitroanilide was monitored at 405 nm.

Western blot analysis

After treatments, cells were rinsed with PBS, scraped, and centrifuged. The pellet was resuspended in 80 μl of RIPA buffer (Uranga et al. 2013). Samples were exposed to one cycle of freezing and thawing, incubated at 4 °C for 60 min, and centrifuged (10,000×g for 20 min). The supernatant was decanted and lysates containing 25–50 μg protein were separated by reducing 10% polyacrylamide gel electrophoresis and electroblotted to polyvinylidene difluoride membranes. Membranes were blocked with 5% nonfat dry milk in TBS-T buffer for 1 h at RT and then incubated with primary antibodies (Cell Signaling Technology) overnight at 4 °C, washed three times with TBS-T, and then exposed to the HRP-conjugated secondary antibody for 1 h at RT. Membranes were washed three times with TBS-T and immunoreactive bands were detected by enhanced chemiluminescence (ECL, GE Healthcare Bio-Sciences) using standard X-ray film. Immunoreactive bands of three independent experiments were quantified using image analysis software (ImageJ, a freely available application in the public domain for image analysis and processing, developed and maintained by Wayne Rasband at Research Services Branch, National Institute of Mental Health, USA).

Immunofluorescence microscopy

IMR-32 cells were grown onto glass coverslips and treated with 10–25 μM **5** for 24 h. They were fixed with 4% paraformaldehyde for 20 min at RT, followed by several washes with PBS, 30 mM glycine/PBS (pH 7.4), and PBS again. For immunostaining, cells were permeabilized and nonspecific sites were blocked with 5% BSA/0.3% Triton X-100/PBS (pH 7.4) at RT for 1 h. After 1 h incubation at RT with the appropriate primary antibody (1:50 in 1% BSA/0.3% Triton X-100/PBS), cells were washed three times with PBS and incubated with the appropriate Alexa Fluor® 488-conjugated secondary antibody (1:200 in 1% BSA/PBS; 1 h at RT) and Hoechst for nuclear staining. After washing with PBS, coverslips were mounted and slides were observed with a Nikon Eclipse E-600 microscope. Quantification was performed using ImageJ and at least 50 cells of three independent experiments were analyzed.

Statistical analysis

Values were expressed as the mean ± SD. Results were analyzed by one-way analysis of variance (ANOVA) to determine group differences, followed by Tukey's post hoc analysis to determine specific differences between conditions. Statistical significance for all analyses was accepted at $p < 0.05$, and *, **, and *** represent $p < 0.05$, $p < 0.01$, and $p < 0.001$, respectively. Western blots and immunocytochemistry images are representative of at least three analyses performed on samples from at least three separate experiments.

Results

Chemistry

17-Hydroxycativic acid (**1**) is a labdane diterpenoid isolated from the aerial parts of *G. ventanensis* as previously described (Alza et al. 2014). To analyze additional properties of semisynthetic derivatives of **1**, we synthesized hybrids of this privileged structure and natural phenols using the Mitsunobu protocol (Appendino et al. 2002), a highly chemoselective esterification method. Ester **3** was obtained from **1** and coniferyl alcohol, whereas esters **4** and **5** were prepared from the methyl ester of **1** (**2**) and ferulic acid and caffeic acid, respectively (Fig. 1). All compounds were rigorously characterized by NMR spectroscopy and mass spectrometry (Supplementary information). Hybrids **3**–**5** are described here for the first time and 2D NMR spectra were used for the unequivocal assignments (Table 1).

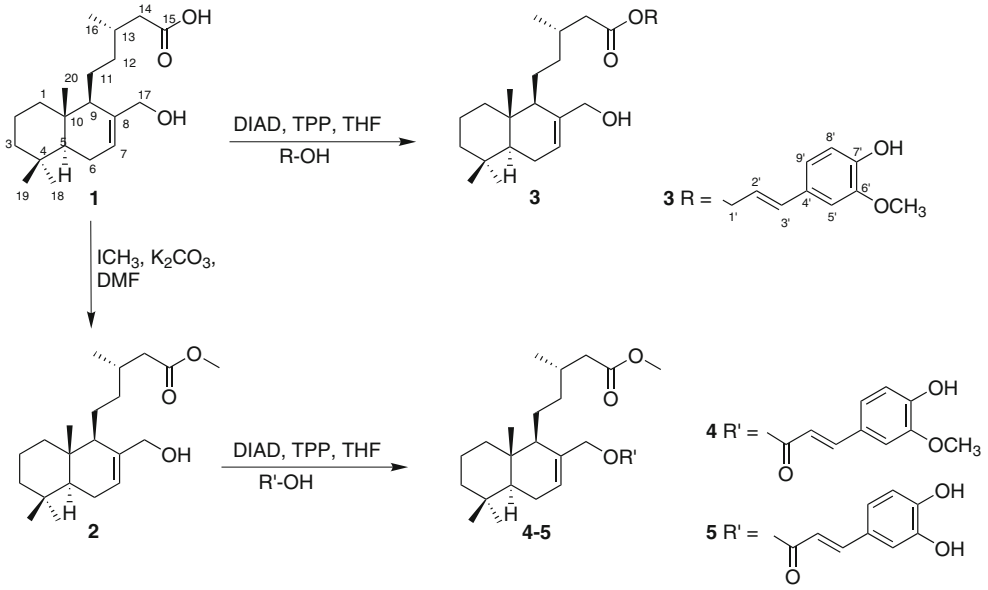

Fig. 1 Semisynthesis of hybrids **3**–**5** through Mitsunobu esterification

Effect of cativic acid hybrids on IMR-32 cell viability

In order to analyze the effects of **1** and hybrids **3**–**5** on cell growth, cell viability of the IMR-32 cell line was assessed using the MTT reduction assay (Uranga et al. 2013). Paclitaxel was used as a positive control (IC_{50} = 2.3 ± 0.2 μM). IMR-32 is a cell line derived from human neuroblastoma and established from an abdominal mass occurring in a 13-month-old male. Diterpenoid **1** and natural phenols (coniferyl alcohol, ferulic acid, or caffeic acid) yielded no effect on cell viability even after 72 h of treatment (Fig. 2a, b). Hybrid **3** did not affect cell viability at the tested concentrations (Fig. 2c). As shown in Fig. 2d, after 72 h of treatment, compound **4** reduced cell growth at 25 and 50 μM but increased cell viability at concentrations in the range of 0.5–10 μM. Compound **5** inhibited cell growth in a dose- and time-dependent manner (Fig. 2e, f), showing the most potent inhibitory effect against IMR-32 cell growth, with an IC_{50} value of 18.0 ± 1.3 μM. Similar results were observed in relation to the viability of cancer cell lines HCT116 and MDA-MB 231 as well as of human embryonic kidney HEK 293 cells after treatment with **5** for 72 h (Table 2). Taking into account these results, the potential mechanisms involved in the biological effect displayed by hybrid **5** were further studied.

Characterization of cell death after hybrid 5 exposure

To characterize the cytotoxic effect of hybrid **5** on human neuroblastoma IMR-32 cells, the probe SYTOX green (permeant to compromised membranes characteristic of dead cells) was used. Treatment with **5** (10–25 μM) increased the number of dead cells in a dose-dependent manner (Fig. 3a). In addition, the number of total nuclei, analyzed with Hoechst, decreased at both concentrations of hybrid **5** (Fig. 3b) in correlation with the results derived from the MTT assay. In line with these findings, IMR-32 cells exposed to **5** (25 μM) increased LDH leakage, an indicator of cell membrane permeability, whereas 10 μM **5** had no effect compared to the control condition (Fig. 3c). In order to determine whether the biological effect of hybrid **5** also implied apoptotic death, activation of caspase-3, a crucial player in apoptosis that cleaves most of caspase-related substrates, was evaluated. As shown in Fig. 3d, caspase-3 activity was significantly higher (1.5-fold) in **5**-exposed conditions with respect to control conditions. In order to reinforce these results, we also checked the presence of cleaved caspase-3 by immunocytochemistry at two different concentrations of **5** (Fig. 3e). The increase of the cleaved caspase-3 levels was in accordance with the enhancement in the enzyme activity observed at 10 and 25 μM **5**.

To assess the mechanism involved in the decrease of cell viability triggered by hybrid **5**, we performed the MTT assay in the presence of the antioxidant *N*-acetylcysteine (NAC). NAC was able to partially prevent the reduction in IMR-32 cell viability exerted by **5**, thus suggesting that the production of reactive oxygen species could be responsible for its biological activity (Fig. 3f). To further characterize the events involved in the toxicity of **5**, log *P* values were calculated to estimate membrane penetrance. As observed in Fig. 3g, hybrid **5** presented the highest log *P* value compared to its constituent monomers. These results suggest that **5** has enhanced membrane penetration.

Effect of hybrid 5 on cell proliferation

To further study the biological effects of hybrid **5**, we next investigated cell proliferation status by using the BrdU assay. Figure 4a shows that exposure to **5** (10, 15, and 20 μM) decreased the number of BrdU-positive cells relative to untreated cells after 12 and 24 h of incubation. The antiproliferative effect was dependent on hybrid **5** concentration. Considering the effect

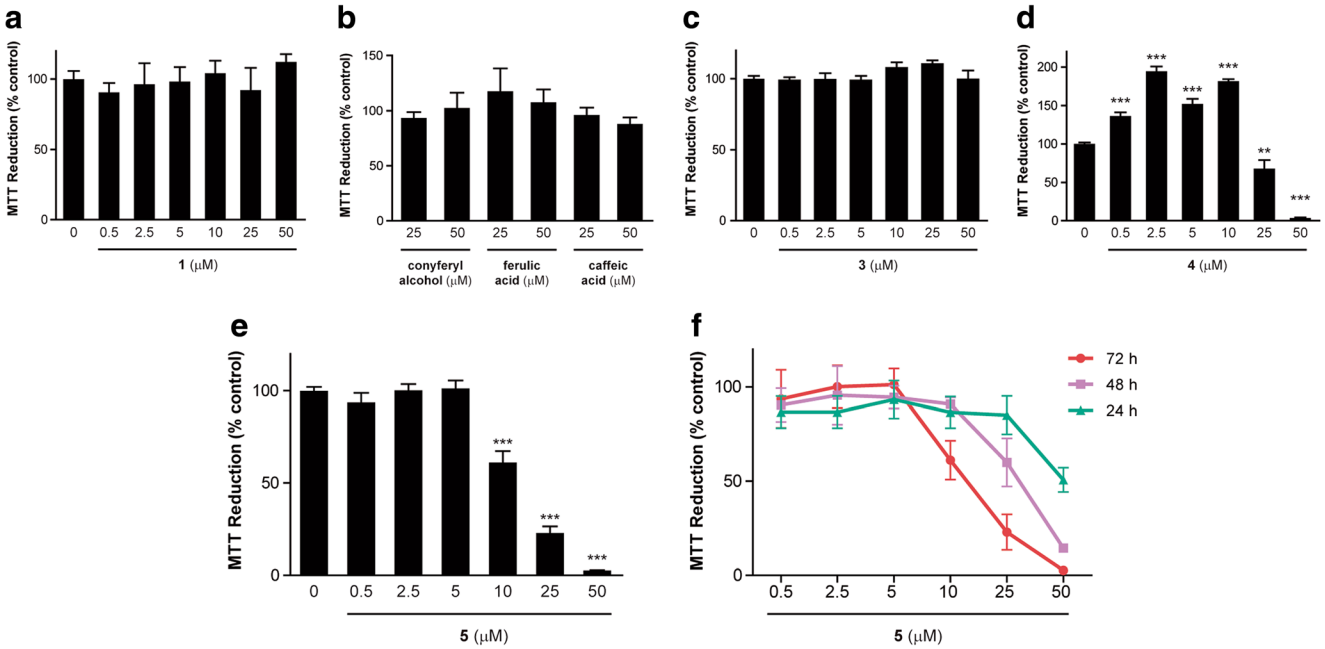

Fig. 2 Effect of 17-hydroxycativic acid (**1**) and hybrids **3**–**5** on viability of human neuroblastoma cells. IMR-32 cells were treated with different concentrations of **1** (**a**), natural phenols (**b**) and hybrids **3** (**c**), **4** (**d**), and **5** (**e**) for 72 h, and for 24 and 48 h for **5** (**f**). Cell viability was assessed by MTT reduction assay. Data are shown as means ± SD (three replicates of three independent experiments)

of **5** on cell proliferation, we next analyzed cell cycle distribution of human neuroblastoma cells by flow cytometry with detection of PI-stained DNA. IMR-32 cells were treated with two concentrations of **5** (10 and 20 μM) for 24 and 72 h. Figure 4b shows that treatment with **5** induced a differential cell cycle distribution which showed to be dependent on the concentration of **5** and the time of incubation. An increase in the S phase population was observed at 10 μM **5** only after 72 h of incubation. At 20 μM **5**, we observed an arrest in S phase after 24 and 72 h of incubation. G2/M phase population was also increased at 20 μM **5** after 72 h of incubation, with a consequent decrease in the G0/G1 phase. The appearance of sub-G0/G1 phase was evident when the cells were treated with **5** at all the assayed concentrations. Thus, treatment of IMR-32 cells with hybrid **5** not only induced cell cycle changes but also triggered apoptotic cell death.

Signaling pathways involved in hybrid 5 cellular effects

To shed more light on the biological effect of hybrid **5**, we next investigated the state of MAPK signaling: signal regulated kinase 1 and 2 (ERK1/2) and c-Jun NH2 terminal kinase (JNK).

Table 2 Effect of hybrid **5** on the viability of different cell lines

Cell line	IC_{50} (μM)
IMR-32	18.0 ± 1.3
HCT-116	22.9 ± 1.5
MDA-MB-231	16.0 ± 2.3
HEK 293	25.8 ± 1.3

ERK1/2 phosphorylation levels were higher in IMR-32 cells exposed to **5** (10–25 μM) for 12 and 24 h (Fig. 5a). Additionally, ERK1/2 activation was accompanied by their cellular redistribution after treatment with **5**. As shown in Fig. 5b, c, compound **5** triggered ERK1/2 translocation from the cytosol to the nucleus and increased c-Jun nuclear content compared to the control condition.

Cell viability in the presence of specific inhibitors of ERK1/2 and JNK was also analyzed. IMR-32 cells were pre-incubated with either ERK 1/2 inhibitor, U0126 (10 μM), or JNK inhibitor, SP600125 (10 μM), and then subsequently treated with 10–25 μM **5** for 72 h. Both MAPK inhibitors, U0126 and SB600125, reduced cell viability compared with hybrid **5** treatment alone (Fig. 5d).

Discussion

Labdane diterpenoids are a large class of NP mainly distributed among higher plants within botanical families such as Labiatae, Asteraceae, Acanthaceae, Euphorbiaceae, Chloranthaceae, and Zingiberaceae (Frija et al. 2011). A variety of bioactivities has been attributed to labdanes, including anti-inflammatory, antibacterial, antifungal, antiprotozoal, cytotoxic, cardiotonic, antiviral, enzyme inducing, and hypotensive activities and modulation of immune cell functions (Frija et al. 2011; Demetzos and Dimas 2001). Few labdane hybrids have been reported in the literature. Pseudolaridimers A and B, isolated from the cones of *Pseudolarix amabilis*, were formed via a [4 + 2] Diels-Alder cycloaddition between a

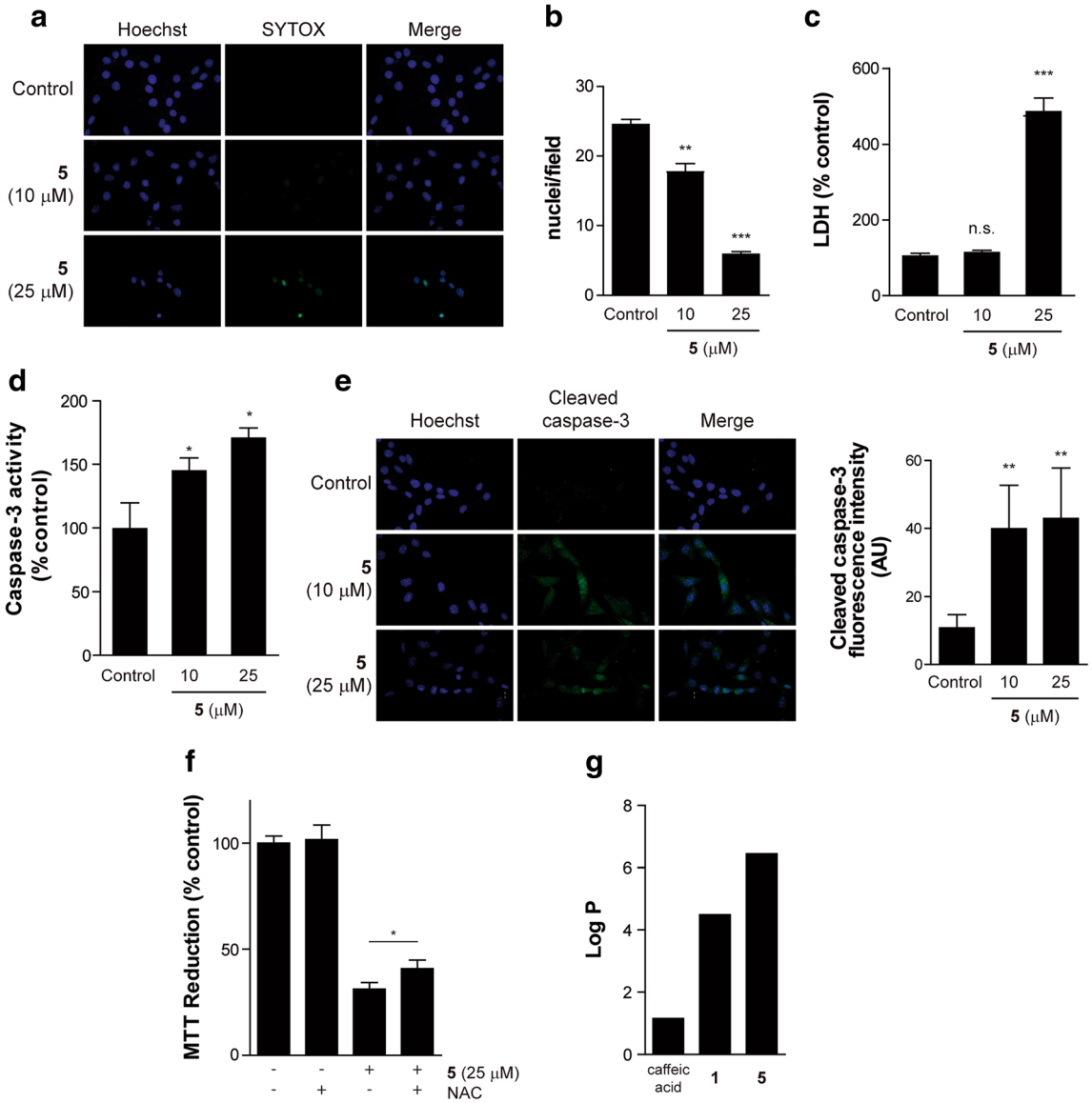

Fig. 3 Cytotoxic effect of hybrid **5** and activation of caspase-3. **a** SYTOX green staining of IMR-32 cells. Cells were incubated with **5** (10–25 μM) or its vehicle overnight, and nuclei were stained with Hoechst (nuclear marker) and SYTOX green (marker of dead cells). **b** Number of nuclei per field counted from the above-described assay (means ± SD; $^{**}p < 0.01$, $^{***}p < 0.001$). **c** LDH leakage assay was assessed in cells after exposure to the same conditions described in **a**. Results are expressed as a percentage of the control. Three independent experiments were performed (mean ± SD; $^{***}p < 0.001$). **d** Caspase-3 activation in hybrid **5**-treated cells was measured spectrophotometrically and results are shown as a percentage of the control (mean ± SD; $^{*}p < 0.05$). **e** Immunocytochemistry studies were performed using the antibody against cleaved caspase-3 in IMR-32 cells after **5** exposure. Hoechst was used as nuclear marker. One representative image of at least three different experiments is presented. Fluorescence intensity quantification is presented in the graph on the right (mean ± SD; $^{**}p < 0.01$ with respect to the control). **f** MTT reduction assay. IMR-32 cells were incubated with the antioxidant *N*-acetylcysteine (1 mM) or its vehicle for 60 min and then treated with **5** (25 μM) or its vehicle, and cell viability was assessed (three replicates of three independent experiments). Results represent mean ± SD ($^{*}p < 0.05$). **g** Log *P* values predicted using ChemDraw Ultra

cycloartane triterpenoid and a labdane. These compounds, particularly pseudolaridimers A, were found to reduce the viability of HCT-116, ZR-75-30, and HL-60 cell lines with IC_{50} values of 9.62, 7.84, 8.29 μg/ml, respectively (Li et al. 2012). Semisynthetic dimers of labdane imbricatolic acid, prepared using esters, ethers, and the triazole ring as linkers (Pertino et al. 2013), were able to reduce the viability of HL-60 and AGS human tumor cell lines.

We have previously described the acetylcholinesterase inhibition in vitro displayed by derivatives obtained from a bioactive labdane (**1**) isolated from *G. ventanensis*. These compounds were prepared by connecting the diterpenoid scaffold with tertiary amine groups through carbon spacers of different lengths, resulting in compounds with enhanced acetylcholinesterase inhibitory activity (Alza et al. 2014).

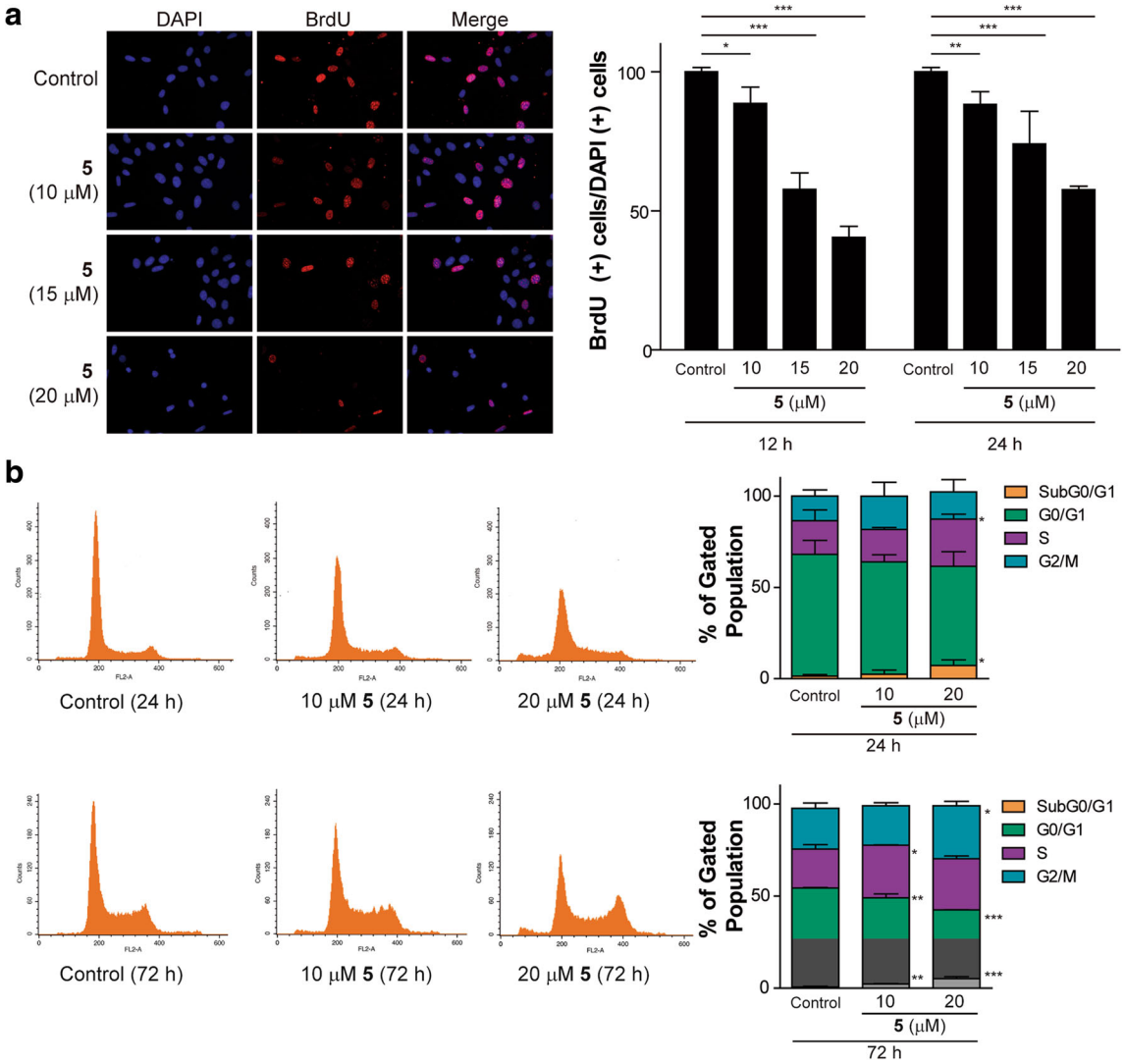

Fig. 4 Effect of hybrid **5** on human neuroblastoma cell proliferation. **a** Cell proliferation was analyzed by BrdU incorporation assay after exposure to **5** (10, 15, and 20 μM) or its vehicle for 12 and 24 h. Images show the results after 24 h of incubation. Nuclei were stained with DAPI. Three independent experiments were performed. Percentage of BrdU-positive cells with respect to DAPI positive cells is represented in the right panel (means ± SD; $*p < 0.05$, $**p < 0.01$, $***p < 0.001$). **b** Cell cycle analysis of IMR-32 cells. After treatments, cells were stained with PI and stained DNA was detected by flow cytometry. The data in the histograms are representative of three independent experiments. Bar plot represents percentage of cell population in sub-G0/G1, G0/G1, S, and G2/M phases (means ± SD; $*p < 0.05$, $**p < 0.01$, $***p < 0.001$)

In this work, we characterized the biological effect of cativic acid hybrids obtained from conjugation with phenols. Our results indicate that hybrids **4** and **5** have different biological properties with respect to their monomers, as was previously reported for the naturally occurring hybrids cephalostatins and ritterazines (Tietze et al. 2003). Hybrid **5** is more bioactive than its constituent monomers (compound **1** and caffeic acid). Although anticancer properties have been reported for caffeic acid and cinnamic acid derivatives (De et al. 2011), no reduction of viability was observed when IMR-32 cells were treated with this phenolic compound. It can be hypothesized that the labdane moiety of **5** improves cell permeability, as estimated by the log *P* values prediction, thus enhancing growth inhibitory activity. Similarly, other natural and synthetic esters of cinnamoyl moieties have shown anticancer activity (De et al. 2011; Li et al. 2015). Taking into account that the **5** IC_{50} value is in the micromolar range and that the desirable concentration for anticancer agents is in the nanomolar range, hybrid **5** could constitute a promising template for developing more potent derivatives.

Additional characterization of hybrid **5** showed that this compound is able to induce cytotoxicity through an increase in cell membrane permeability and to trigger apoptotic cell death. Caspase-3 activation and the increased levels of cleaved caspase-3 were accompanied by an antiproliferative effect in human neuroblastoma cells exposed to hybrid **5**.

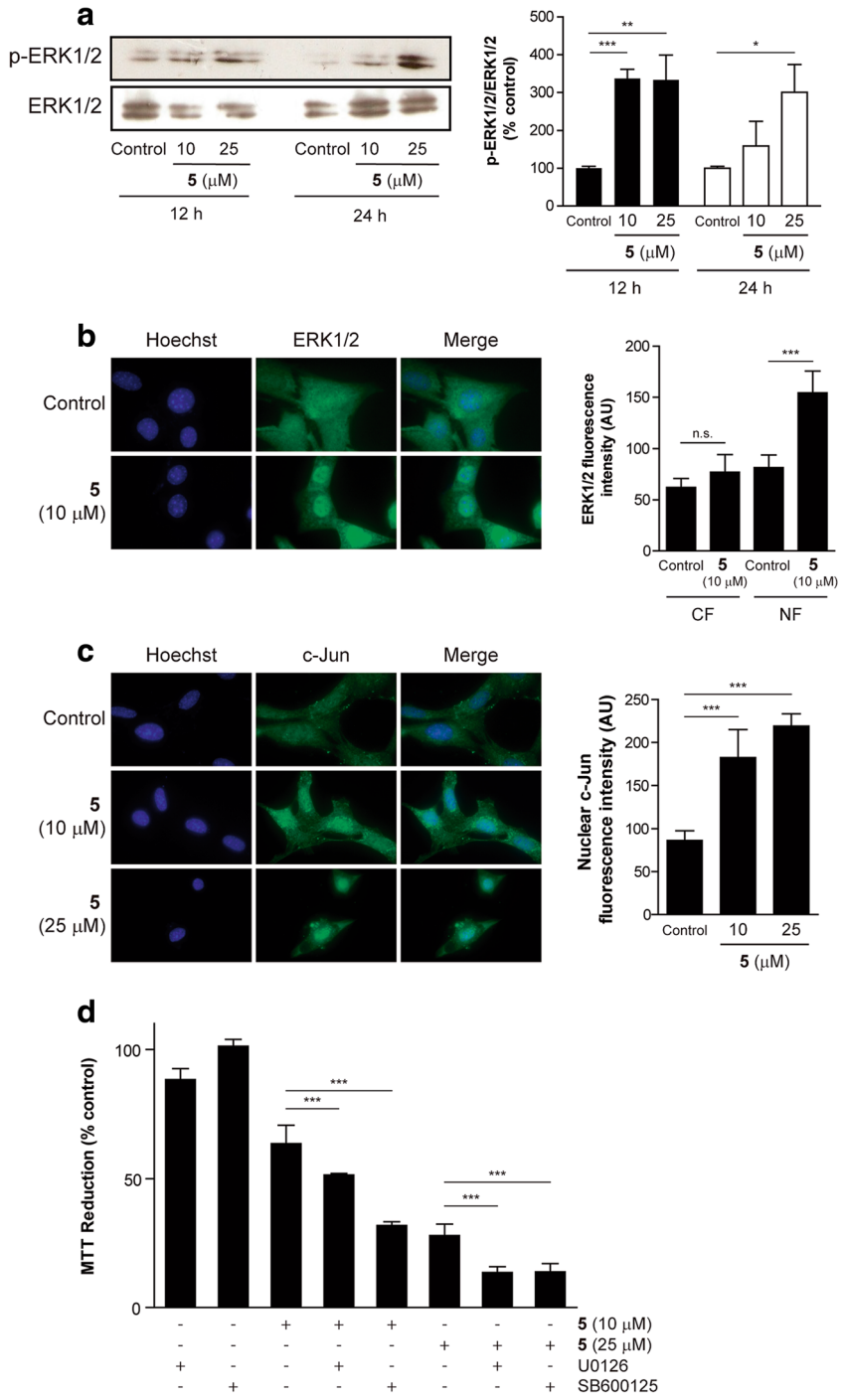

Fig. 5 Enhancement of growth inhibitory effect of hybrid **5** through MAPK pathway inhibition. **a** ERK 1/2 phosphorylation was assessed by Western blot assays of IMR-32 cells exposed to **5** (10–25 μM) for 12 and 24 h. One blot image representative of three different experiments is shown. The data in the graph on the right represent the ratio between p-ERK1/2 and ERK1/2 (percentage of the control condition; mean ± SD of three independent experiments) using scanning densitometry for protein band quantification (*$p < 0.05$, **$p < 0.01$, ***$p < 0.001$ with respect to the control). **b** Intracellular distribution of ERK1/2 was determined by immunocytochemistry studies in cells treated with hybrid **5** (10 μM) or its vehicle. **c** After treatments, IMR-32 cells were processed for immunocytochemistry using antibody against c-Jun. **b**, **c** Hoechst was used as a nuclear marker. One representative blot image of three different experiments is shown. The data in the graphs on the right represent fluorescence intensity (mean ± SD of three independent experiments; ***$p < 0.001$ with respect to the control, n.s. = no significant difference). CF = cytosolic fraction; NF = nuclear fraction. **d** MTT reduction assay. IMR-32 cells were treated with U0126 (ERK1/2 inhibitor) and SB600125 (JNK inhibitor) or their vehicles for 30 min, and then exposed to **5** (10–25 μM) or its vehicle, and cell viability was assessed (three replicates of three independent experiments). Results represent mean ± SD (***$p < 0.001$)

Different anticancer agents have been shown to inhibit cell proliferation through activation of many signaling pathways that arrest the cell cycle at the G0/G1, S, or G2/M phase; at a particular checkpoint, this arrest drives cancer cells to death (Khan et al. 2015). We found that compound **5** suppressed cell proliferation through a differential cell cycle distribution depending on its concentration and incubation time.

Alterations in the expression or activity of ERK1/2 and JNK have different functions related to tumorigenesis or cancer progression. Modulation of these pathways has been an attractive target for cancer therapy although their effects depend on the tumor type (Dhillon et al. 2007). Our results reveal that ERK1/2 and JNK activation is a protective mechanism used by cells to counter the effect induced by hybrid **5**, thus suggesting that inhibition of both MAPK potentiates the growth inhibitory effect of **5** in the IMR-32 cell line. Similar results were obtained with some anticancer agents in other cancer cell lines. Temozolomide, a drug approved to treat anaplastic astrocytoma

and multiform glioblastoma, displays potential cytotoxicity under conditions of JNK inhibition in the glioma cell line U87MG (Vo et al. 2014). Adriamycin-induced apoptosis in leukemia cells HL-60 is enhanced by ERK1/2 inhibition (Zhou et al. 2010). It has also been shown that ERK1/2 inhibitor PD98059 synergistically potentiates the ability of trichostatin A to mediate cell cycle arrest and apoptosis of gastric carcinoma cell line SGC7901 (Yao et al. 2012). Regarding the activity of MAPK downstream transcription factors, it has been extensively reported that the increase in c-Jun nuclear localization leads to apoptosis or changes in differentiation (Schreck et al. 2011). Coincidentally, the rise in c-Jun nuclear content in the presence of hybrid **5** reinforces its role as apoptotic modulator.

Conclusions

Taken together, our results show that compound **5**, derived from the esterification of caffeic acid with the natural labdane cativic acid, has the ability to trigger antiproliferative signals and apoptosis in human neuroblastoma cells. These biological effects are exclusive to this hybrid, since its monomers have no biological effects. Our study also suggests that ERK1/2 and JNK inhibition enhances the growth inhibitory effect of hybrid **5** on neuroblastoma cells. These findings could pave the way for further studies aimed at a better understanding of the biological activity of cativic acid hybrids in cell proliferative disorders.

Acknowledgements The authors wish to thank Wiener Laboratories for kindly providing LDH kits. They also gratefully acknowledge Dr. Maria Marta Facchinetti and Dr. Alejandro Curino for kindly providing HCT-116 and MDA-MB-231 cancer cell lines and Dr. I. Luthy for a sample of paclitaxel. NPA is a post-doctoral fellow of CONICET. GAS and APM are research members of CONICET. The funders had no role in the study design, data collection and analysis, decision to publish, or preparation of this manuscript.

Funding information This work was supported by the Agencia Nacional de Promoción Científica y Tecnológica (ANPCyT) (PICT-2013-0987 and PICT-2011-0765), Consejo Nacional de Investigaciones Científicas y Técnicas (CONICET) (PIP1122009010068 and PIP11220100100392), and the Universidad Nacional del Sur (UNS) (PGI24B179 and PGI24Q071) to GAS and to APM, respectively.

References

Ahmed A, Mahmoud A, Ahmed U, El-Bassuony A, Abd El Razk M, Pare P et al (2001) Manoyl oxide alpha-arabinopyranoside and grindelic acid diterpenoids from *Grindelia integrifolia*. J Nat Prod 64:1365–1367

Alza NP, Richmond V, Baier CJ, Freire E, Baggio R, Murray AP (2014) Synthesis and cholinesterase inhibition of cativic acid derivatives. Bioorg Med Chem 22:3838–3849

Appendino G, Minassi A, Daddario N, Bianchi F, Tron GC (2002) Chemoselective esterification of phenolic acids and alcohols. Org Lett 4:3839–3841

Berube G (2016) An overview of molecular hybrids in drug discovery. Expert Opin Drug Discov 11:281–305

Bradford MM (1976) A rapid and sensitive method for the quantitation of microgram quantities of protein utilizing the principle of protein-dye binding. Anal Biochem 72:248–254

De P, Baltas M, Bedos-Belval F (2011) Cinnamic acid derivatives as anticancer agents—a review. Curr Med Chem 18(11):1672–1703

Demetzos C, Dimas KS (2001) Studies in natural products chemistry. Elsevier, Oxford [Bioactive Natural Products]

Dhillon AS, Hagan S, Rath O, Kolch W (2007) MAP kinase signalling pathways in cancer. Oncogene 26:3279–3290

Frija LM, Frade RF, Afonso CA (2011) Isolation, chemical, and biotransformation routes of labdane-type diterpenes. Chem Rev 111:4418–4452

Hanzel CE, Verstraeten SV (2009) Tl(I) and Tl(III) activate both mitochondrial and extrinsic pathways of apoptosis in rat pheochromocytoma (PC12) cells. Toxicol Appl Pharmacol 236:59–70

Hoffmann JJ, Jolad SD, Timmermann BN, Bates RB, Camout FA (1988) Two grindelane diterpenoids from Grindelia camporum. Phytochemistry 27:493–496

Khan M, Maryam A, Qazi JI, Ma T (2015) Targeting apoptosis and multiple signaling pathways with icariside II in cancer cells. Int J Biol Sci 11:1100–1112

Li B, Kong DY, Shen YH, Yuan H, Yue RC, He YR et al (2012) Pseudolaridimers A and B, hetero-cycloartane-labdane Diels-Alder adducts from the cone of Pseudolarix amabilis. Org Lett 14:5432–5435

Li L, Zhao P, Hu J, Liu J, Liu Y, Wang Z et al (2015) Synthesis, *in vitro* and *in vivo* antitumor activity of scopoletin-cinnamic acid hybrids. Eur J Med Chem 93:300–307

Mahmoud A, Ahmed A, Tanaka T, Iinuma M (2000) Diterpenoid acids from *Grindelia nana*. J Nat Prod 63:378–380

Newman DJ, Cragg GM (2016) Natural products as sources of new drugs from 1981 to 2014. J Nat Prod 79:629–661

Pertino MW, Theoduloz C, Bastias M, Schmeda-Hirschmann G (2013) Dimeric labdane diterpenes: synthesis and antiproliferative effects. Molecules 18:5936–5953

Schreck I, Al-Rawi M, Mingot J, Scholl C, Diefenbacher M, O'Donnell P et al (2011) c-Jun localizes to the nucleus independent of its phosphorylation by and interaction with JNK and vice versa promotes nuclear accumulation of JNK. Biochem Biophys Res Commun 407:735–740

Tietze LF, Bell HP, Chandrasekhar S (2003) Natural product hybrids as new leads for drug discovery. Angew. Chem Int Ed Engl 42:3996–4028.a

Uranga RM, Giusto NM, Salvador GA (2009) Iron-induced oxidative injury differentially regulates PI3K/Akt/GSK3 beta pathway in synaptic endings from adult and aged rats. Toxicol Sci 111:331–344

Uranga RM, Katz S, Salvador GA (2013) Enhanced phosphatidylinositol 3-kinase (PI3K)/Akt signaling has pleiotropic targets in hippocampal neurons exposed to iron-induced oxidative stress. J Biol Chem 288:19773–19784

Vo VA, Lee JW, Lee HJ, Chun W, Lim SY, Kim SS (2014) Inhibition of JNK potentiates temozolomide-induced cytotoxicity in U87MG glioblastoma cells via suppression of Akt phosphorylation. Anticancer Res 34:5509–5515

Yao J, Qian CJ, Ye B, Zhang X, Liang Y (2012) ERK inhibition enhances TSA-induced gastric cancer cell apoptosis via NF-kappaB-dependent and Notch-independent mechanism. Life Sci 91:186–193

Zhou L, Luan H, Dong X, Li Y (2010) Activation of the PI3K/Akt and MAPK signaling pathways antagonizes adriamycin-induced HL-60 leukemia cell apoptosis. Mol Med Rep 3:641–644

Zuloaga FO, Morrone O, Belgrano MJ, Marticorena C, Marchesi E (2008) Catálogo de las Plantas Vasculares del Cono Sur (Argentina, Sur de Brasil, Chile, Paraguay y Uruguay). St. Louis, Missouri Botanical Garden